ARTICLE

Electrochemical Charging of Individual Single-Walled Carbon Nanotubes

Martin Kalbac,[†,§,*] Hootan Farhat,[‡] Ladislav Kavan,[†] Jing Kong,[§] Ken-ichi Sasaki,[∥] Riichiro Saito,[¶] and Mildred S. Dresselhaus[§,⊥]

[†]J. Heyrovský Institute of Physical Chemistry, Academy of Sciences of the Czech Republic, v.v.i., Dolejškova 3, CZ-18223 Prague 8, Czech Republic, [‡]Department of Materials Science and Engineering, Massachusetts Institute of Technology, Cambridge, Massachusetts 02139, [§]Department of Electrical Engineering and Computer Science, Massachusetts Institute of Technology, Cambridge, Massachusetts 02139, [∥]National Institute for Materials Science, Namiki, Tsukuba 305-0044, Japan, [¶]Department of Physics, Tohoku University, Sendai 980-8578, Japan, and [⊥]Department of Physics, Massachusetts Institute of Technology, Cambridge, Massachusetts 02139

ABSTRACT The influence of the electrode potential on the electronic structure of individual single-walled carbon nanotubes is studied using Raman spectroscopy. By analyzing the radial breathing mode intensity *versus* electrode potential profiles in the Raman spectra at many different laser excitation energies, we show that the charging of individual carbon nanotubes causes a broadening of the resonant Raman profiles (resonance window). This effect is observed for both a semiconducting and a metallic tube. The broadening of the resonance Raman profiles already begins at potentials where the first electronic states of a particular tube are filled or depleted. The important consequence of this effect is a striking difference between the Raman intensity *versus* potential profiles of metallic and semiconducting tubes. While for a metallic tube the intensity of the Raman signal is attenuated at potentials which deviate slightly from 0 V, for a semiconducting tube, the Raman intensity is significantly attenuated only after the electrode potential reaches the first van Hove singularity. Furthermore, for the metallic tube, a strong asymmetry is found in the bleaching of the Raman signal with respect to positive and negative potentials, which results from the different energy bandwidth for the π^* band and the π band.

KEYWORDS: single-walled carbon nanotubes · Raman spectroscopy · electrochemical gating · spectroelectrochemistry

A fundamental understanding of the changes of the electronic structure of single-walled carbon nanotubes (SWCNTs) due to doping is crucial for tuning their properties to fit specific applications. Therefore, the doping of SWCNTs has been intensively studied for several years.[1−8] *In situ* Raman spectroelectrochemistry is a well-established method for investigating the change in the physical properties of SWCNTs during charging.[9] We have shown previously that electrochemical charging has a strong effect on perturbing the Raman spectra of SWCNT bundles.[9] It is important to distinguish between electrochemical charging and chemical doping. In the latter case, the redox-active molecule (chemical dopant) can penetrate into the interior of carbon nanostructures. In some cases (for example, in fullerene peapods),[10] the chemical doping is highly irreversible and the chemical dopant cannot be completely removed even by extraction with a solvent. Electrochemical charging, on the other hand, mimics a double layer capacitor,[9] where the charge carriers are injected into the nanotube from the electrode and the electrolyte ions only compensate the injected charge.

The main features of the Raman spectra of SWCNTs are the radial breathing mode (RBM), the disorder-induced mode (D), the tangential modes (G^+ and G^-), and the double resonance mode (G′) occurring between 2600 and 2700 cm^{-1}.[11,12]

The RBM band is of particular importance since its frequency scales with inverse tube diameter d_t according to the relation

$$\omega_{RBM} = C_1/d_t + C_2 \qquad (1)$$

where the constant C_1 has been recently reported to be in the range of 217 to 227 $cm^{-1} \cdot nm$ (refs 13 and 14). The constant C_2 (~15 cm^{-1}) is generally used to include the effect of interactions between nanotubes in bundled samples, and therefore, in the case of individual isolated tubes, we expect $C_2 \approx 0$ cm^{-1}. For small diameter tubes, the knowledge of the diameter and resonance profile is sufficient to determine the chiral indicies (*n*,*m*) of the particular nanotubes. All other Raman modes for SWCNTs give relatively little information which can be used for their (*n*,*m*) assignment. Thus, in most Raman studies of SWCNTs, only the RBM band is used to assign the tube (*n*,*m*) indices, and this information is then used for the interpretation of the chirality dependence of other Raman modes.

Despite the large effort put into studies on SWCNT doping, this process is not yet well understood. In previous studies,[6,9,15,16] *in situ* spectroelectrochemical measurements have been typically performed on

*Address correspondence to kalbac@jh-inst.cas.cz.

Received for review April 29, 2009 and accepted July 27, 2009.

Published online July 31, 2009. 10.1021/nn9004318 CCC: $40.75

samples containing large bundles of SWCNTs, which complicated the interpretation of the results, since the individual properties of specific tubes are then averaged. Furthermore, nanotubes in a bundle have been shown to exhibit different properties as compared to those of individual nanotubes.[17] Therefore, it is desirable to focus attention on spectroelectrochemical studies of small bundles and ideally of individual isolated carbon nanotubes.[2,18,19]

The Raman spectra of SWCNTs are resonantly enhanced.[20] This allows detection of a Raman signal even from individual SWCNTs. However, due to the one-dimensional character of SWCNTs, the resonance enhancement may be strongly influenced by the nanotube environment,[21] which complicates the use of Raman spectroscopy in SWCNT metrology. To overcome this problem, it is crucial to study resonance Raman profiles of SWCNTs and the role of the environment in detail. The large variety of possible environments requires a systematic approach which would address the different effects of the environment (such as stress, charge transfer) rather than an empirical study of all possible environments. A charge transfer between the nanotube's surrounding and the SWCNT presumably plays a crucial role. However, a detailed study of the doping effects on nanotube resonance Raman profiles, which would focus on individual tubes, is still a great challenge.

In this paper, we report the effects of electrochemical charging on the RBM band in the Raman spectra of individual semiconducting and metallic SWCNTs. We show experimentally that the Raman intensity *versus* potential profiles is significantly dependent on laser excitation energy, which is a consequence of the change in the resonant Raman profiles at different potentials. We also demonstrate a striking difference between the Raman intensity *versus* potential profiles of metallic and semiconducting tubes as a consequence of their different electronic structure. Our results pave the way for a detailed understanding of the doping process in carbon nanotubes and also explain the observed striking difference between the Raman intensity *versus* potential profiles of metallic and semiconducting carbon tubes.

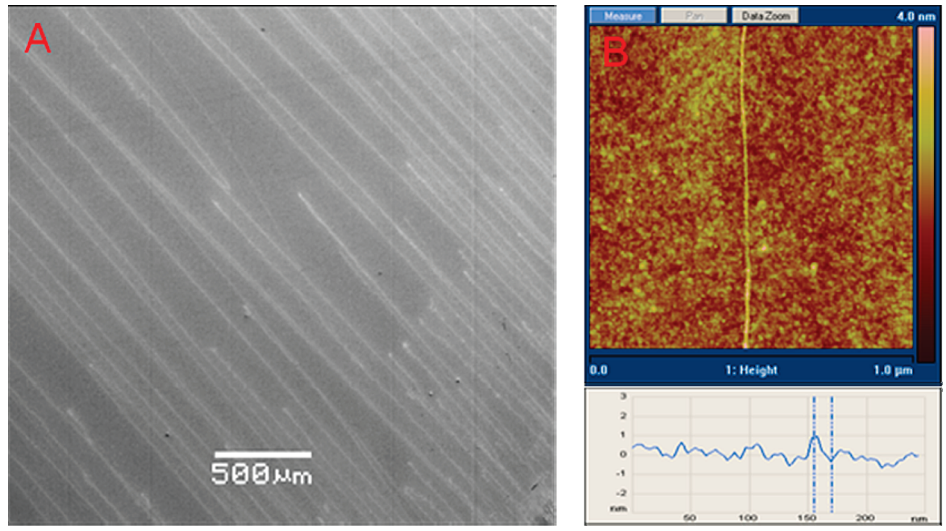

Figure 1. (A) Scanning electron micrograph of the as-grown SWCNTs on a SiO_2/Si substrate. (B) AFM image of an individual tube. The height of the tube is about 1.2 nm.

RESULTS AND DISCUSSION

Figure 1A shows a scanning electron microscope image of SWCNTs grown by chemical vapor deposition (CVD) directly on a SiO_2/Si substrate. The nanotubes in this image are typically parallel to each other and individual, as can be seen in the AFM image (Figure 1B). The distance between adjacent SWCNTs is usually greater than 10 µm. This geometry simplifies finding a tube and also enables alignment of the laser polarization parallel to the SWCNT axis, which is important for obtaining a reasonably strong Raman signal and for establishing a well-defined reproducible geometry for efficient data collection. It is generally difficult to completely exclude the situation where more than one tube is present in the laser spot (0.5 µm in diameter) from which Raman spectra are taken. However, for our analysis, we selected the laser spot where only one RBM band was present. Also, several laser lines were used as probes to ensure that the laser spot does not contain several tubes.

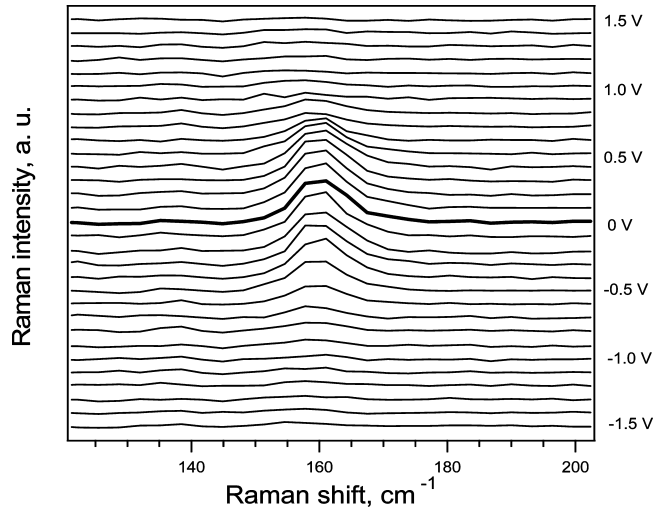

Figure 2. Raman spectra of an individual semiconducting tube (S) at different electrode potentials. The electrode potentials range from −1.5 to 1.5 V *vs* Ag/Ag^+ (from bottom to top). The spectra are excited by 2.102 eV laser excitation energy. The electrochemical potential change between adjacent curves in the figure is 0.1 V, and the spectrum at 0 V is highlighted. The spectra are offset for clarity, but the intensity scale is the same for all spectra.

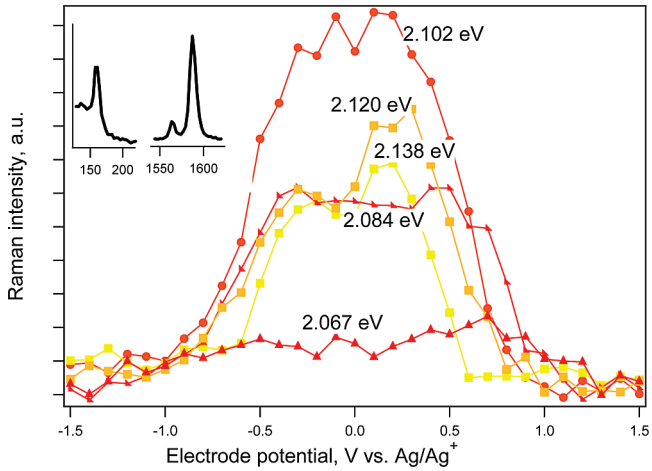

Figure 3. I_{RBM} Raman intensity *vs* potential profiles for the semiconducting tube (S). The Raman spectra were excited using different laser excitation energies, as indicated in the figure. The inset shows the RBM and the tangential mode (G band) regions of the Raman spectra of the studied individual SWCNT at 0 V *vs* Ag/Ag$^+$ for 2.102 eV laser excitation energy.

Figure 2 shows the Raman spectra of an individual semiconducting tube in the RBM frequency ω_{RBM} region at different electrode potentials. The spectra are excited by 2.102 eV laser energy excitation (E_{laser}). The most obvious effect of the electrode potential is a change of the RBM intensity. The small change in ω_{RBM} as a function of electrode potential is discussed elsewhere.[22] The RBM mode in Figure 2 is bleached (or shows a decrease in intensity) as the magnitude of the potential is increased relative to $V_e = 0$ V. The bleaching is observed for both positive and negative electrode potentials V_e, as shown in Figure 2. Note that in our paper we always refer to the electrode potential (V_e) that is applied to the SWCNT which serves as the working electrode. Thus $V_e > 0$ refers to hole doping and $V_e < 0$ is for electron doping.

For a more detailed analysis, we plot the dependence of the Raman intensity of the RBM (I_{RBM}) on the electrode potential in Figure 3. We show in Figure 3 the Raman intensity/potential profiles for the RBM mode of the same semiconducting (S) tube as in Figure 2, but now excited also by other (different) laser excitation energies E_{laser}. The inset of Figure 3 shows the RBM and the tangential mode (G band) region of the Raman spectra of the studied individual SWCNT at 0 V *vs* Ag/Ag$^+$ ($V_e = 0$) for $E_{laser} = 2.102$ eV. The RBM mode frequency ω_{RBM} is about 160 cm^{-1}, which gives a diameter d_t of around 1.42 nm using the equation $d_t = 227/\omega_{RBM}$. We note that there is only one RBM band in the Raman spectra for all probed laser excitation energies and for all potentials. This further confirms that only one individual SWCNT is in the laser spot. The line shape of the lower component G$^-$ of the tangential mode is narrow, which confirms the semiconducting character of the tube. Considering the diameter of the tube to be 1.42 nm, it is suggested by the Kataura plot[23,24] that $E_{laser} = 2.102$ eV is in resonance with the E_{33}^S transition for this nanotube.

The observed dependence of the intensity/potential profile on E_{laser} is shown in Figure 3 for the same semiconducting tube as in Figure 2. The strongest change of the Raman intensity with electrode potential V_e (*i.e.*, the fastest bleaching) is observed if E_{laser} in Figure 3 corresponds to the maximum of the resonance profile (*i.e.*, the spectrum taken with $E_{laser} = 2.102$ eV). On the other hand, if E_{laser} is relatively far from the resonance maximum, the bleaching of the RBM band intensity induced by the electrochemical charging shows only a weak dependence on electrode potential, V_e. This is, for example, the case of the trace for $E_{laser} = 2.067$ eV, where the bleaching of the Raman intensity of the RBM band by the applied electrode potential V_e is almost negligible.

Figure 3 also shows that the bleaching of the Raman intensity of the RBM mode of the semiconducting tube (S) is dependent on the magnitude of the electrode potential V_e. At low electrode potentials (up to a potential of about $\pm$0.5 V), the bleaching of the I_{RBM} shows a relatively weak dependence on V_e. Increasing the magnitude of V_e above $\pm$0.5 V, and up to $\pm$0.8 V, leads to an increased bleaching of the I_{RBM} by the applied V_e. For the magnitude of the electrode potential above about $\pm$0.8 V, the bleaching again decreases slowly with increasing V_e. Finally, at a potential of about $\pm$1.0 V, I_{RBM} reaches the background level (where I_{RBM} is negligible), and thus further bleaching is not observed when the magnitude of the potential is further increased (from $\pm$1.0 to $\pm$1.5 V).

The offset in the start of the bleaching of the Raman signal at low electrode potential ($\pm$0.5 V) can be rationalized by the presence of a band gap in the semiconducting tube. The band gap energy is expected to be about 0.7 eV for the studied semiconducting nanotube. Therefore, the van Hove singularities would be filled/depleted only if the Fermi level E_F is shifted above 0.35 eV or below $-$0.35 eV relative to the neutrality point. Assuming that $V_e = 0$ V corresponds to $E_F = 0$ and a 100% doping efficiency, an electrode potential of V_e above 0.35 V or below $-$0.35 V is needed to fill or deplete the first van Hove singularities in the valence and conduction bands, respectively. The doping efficiency has been shown to be about 50$-$70%,[25] which rationalizes the slightly higher values of the electrode potential that are found necessary to observe bleaching of the Raman signal in our experiment. It is very important to note that the Raman signal of the studied nanotube is enhanced when E_{laser} matches the E_{33}^S excitonic transition, which is here probed by I_{RBM}. The data in Figure 3 make it clear that the filling/depleting of electronic states which correspond to E_{11}^S causes a significant change of I_{RBM}, which is highly sensitive to the E_{33}^S transition. This experimental result is one of the crucial findings of this paper since previous interpreta-

tions of the bleaching assumed that the van Hove singularity which is in resonance with the laser excitation energy (here E_{33}^{S}) must be filled[9] to observe bleaching of the Raman signal. From our present observations, we conclude that our I_{RBM} signal probes the filling and empting of *any* electronic state.

In contrast, Figure 4 shows an example of the Raman intensity *versus* potential profiles for a *metallic* tube (M). Here the Raman spectra were excited using different laser excitation energies ranging from E_{laser} = 1.653 to 1.746 eV, which correspond to the energy interval where this tube is in resonance with E_{laser} (*i.e.*, the resonance window). The inset to Figure 4 shows the RBM and the tangential mode (TG band) regions of the Raman spectra of the studied individual (M) SWCNT at 0 V *vs* Ag/Ag^+ ($V_e = 0$) for E_{laser} = 1.722 eV corresponding to the maximum in I_{RBM}. The G^- component of the TG mode is significantly broadened (inset to Figure 4), which confirms the metallic character of the tube. The RBM peak frequency is close to 160 cm^{-1}. Hence, the diameter of the metallic tube (M) is similar to the diameter d_t of the semiconducting (S) tube shown in Figure 3 ($d_t \approx 1.42$ nm).

For the metallic tube, the bleaching of the I_{RBM} with increasing magnitude of the electrode potential also exhibits a dependence on E_{laser}. The maximum of the resonance profile is close to E_{laser} = 1.722 eV, and thus the bleaching of the I_{RBM} is the fastest as a function of V_e at this laser excitation energy. On the other hand, a negligible bleaching of the I_{RBM} is found for E_{laser} = 1.653 eV (see Figure 4), which is relatively far from the energy corresponding to the resonance maximum.

For the metallic tube, the bleaching of the I_{RBM} is significant already at the beginning of electrochemical charging $V_e = 0$ (for E_{laser} close to the energy of the resonance maximum). This is in contrast to the semiconducting tube (S) where the bleaching of the I_{RBM} only becomes significant for a potential greater than about ±0.35 V. The reason for this difference is that the metallic tube does not have a band gap, and therefore, the electrons may be injected or extracted from electronic states by an infinitesimal shift of the Fermi level away from $E_F = 0$. Note that also for a metallic tube the bleaching of the Raman signal occurs before the Fermi level reaches the first van Hove singularity (E_1^M), which is employed in the resonance enhancement of the Raman signal of the studied metallic tube. In other words, for the metallic tube, the filling of the electronic states close to $E_F = 0$ leads to a significant change in I_{RBM} at E_{11}^M.

Another difference between the metallic tube (Figure 4) and the semiconducting tube (Figure 3) is an asymmetry of the Raman intensity *versus* potential profiles with respect to positive and negative potentials. For the metallic tube, the bleaching of the Raman intensity is faster during charging with positive potentials than during charging with negative potentials. This

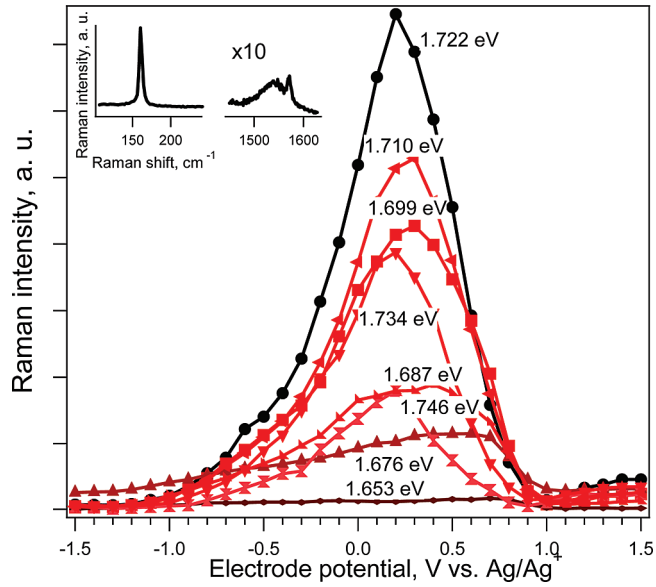

Figure 4. Raman intensity I_{RBM} *vs* potential profiles for a metallic tube (M). The Raman spectra were excited using different laser excitation energies as indicated in the figure. The inset shows the RBM and the tangential mode (TG band) regions of the Raman spectra of the studied individual SWCNT at 0 V *vs* Ag/Ag^+ for E_{laser} = 1.722 eV, where the RBM has maximum intensity.

asymmetry is consistent with the general fact that the density of states for the π* band is smaller (energy bandwidth is larger) than that for the π band. (The difference of the energy band between π and π * comes from the overlap matrix parameter $s = 0.129$ which makes the conduction (valence) bandwidth large (small).)[26] In other words, for the π* band, E_F must be moved more to inject a given amount of carriers than for the π band. The asymmetry may also indicate that the filling of the states with electrons is more difficult (requires a higher magnitude of V_e) than depleting electrons. It is important that this particular asymmetry is not found for the semiconducting tube because it ensures that the asymmetry of the Raman intensity *versus* potential profiles in the case of the metallic tube is not caused by "extrinsic" effects such as the conductivity of the electrolyte or the mobility of the electrolyte ions. Further discussion of the different asymmetries between the S and M tubes is given below. Nevertheless, even for the metallic tube (M), the Raman intensity *versus* potential profiles is broadened if the laser energy is relatively far from the energy corresponding to the resonance maximum, and this effect is, for example, shown for the case of E_{laser} = 1.687 eV in Figure 4. Furthermore, the maximum of the intensity *versus* potential profile is shifted toward higher potentials for laser excitation energies which are relatively far from the energy of the resonance maxima, such as in the case of E_{laser} = 1.676 eV in Figure 4. Similar to the case of the semiconducting tube (S), at a potential V_e of about ±1 V, the I_{RBM} for the metallic tube (M) reaches the background level and the signal is difficult to distinguish from the background. We assume that at a potential V_e of about

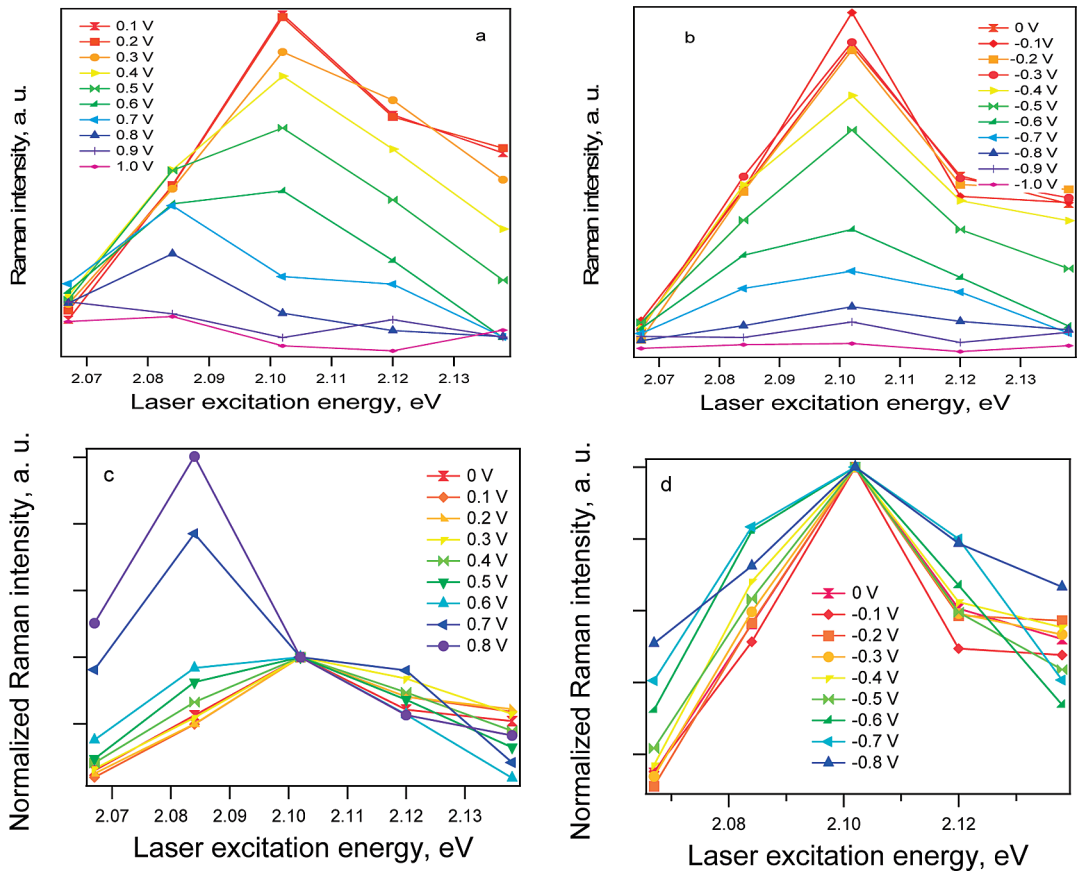

Figure 5. Raman intensity I_{RBM} *vs* laser excitation energy profiles for the semiconducting (S) tube for positive potentials (a) and for negative potentials (b). The normalized Raman intensity I_{RBM} *vs* laser excitation energy profiles for the semiconducting (S) tube for positive potentials (c) and for negative potentials (d), in which the Raman intensity for each curve is normalized to I_{RBM} at 2.102 eV.

$\pm$1 V the E_{11} transition is completely blocked by filling the E_1^M valence sub-band or depleting the E_1^M conduction sub-band.

The Raman resonance profiles for the semiconducting (S) tube at different electrode potentials are shown in Figure 5a,b. We also show these resonance profiles at the same values of V_e in Figure 5c,d, but here the data are normalized to the I_{RBM} at 2.102 eV for each value of V_e.

It is obvious in Figure 5 that the electrode potential significantly influences the resonance Raman I_{RBM}/E_{laser} profiles. It seems visually that increasing the magnitude of the electrode potential causes a broadening of the resonance Raman profile for S tubes in Figure 5. The effect is observed for both positive and negative charging of the semiconducting nanotube. Furthermore, for high positive potentials (0.7 and 0.8 V), where hole doping occurs, there is a shift of the resonance maxima to lower energies. This effect is much less pronounced for negative potentials.

The shift of the resonance maxima may indicate a change in the E_{33}^S transition due to the filling/depleting of states in the E_1^S band. A change of the E_{ii}^S as a consequence of electrochemical doping has been suggested previously.[16] (Note that the filling/depleting of E_3^S was assumed in ref 16.) The consequences of the E_{ii}^S change with E_1^S filling/depleting should also be observed in the spectroelectrochemical behavior of samples containing a broad diameter distribution of SWCNTs. For such a bundle sample and a given laser excitation energy, it is expected that a few tubes will be close to perfect resonance, while other tubes will be within the resonance window, but more or less out of resonance on either side of the resonance maximum. If the E_{ii} changes during the charging of the sample, the signal from tubes in perfect resonance would decrease in intensity. The change of the RBM signal of the tubes slightly off-resonance would depend on the relative position of their E_{ii} with respect to E_{laser}. Since there is a random distribution of (n,m) tubes in the bundled sample, the I_{RBM} of some of these tubes should decrease in intensity and the I_{RBM} of other tubes should increase in intensity as E_{laser} is changed. However, the observed overall signal of the RBM bands for nanotube bundles is typically decreased and no significant increase of I_{RBM} is observed as the magnitude of the electrode potential is increased.[9] Our results on individual nanotubes in the present work indicate that the change in E_{ii}^S with V_e is small, and at the

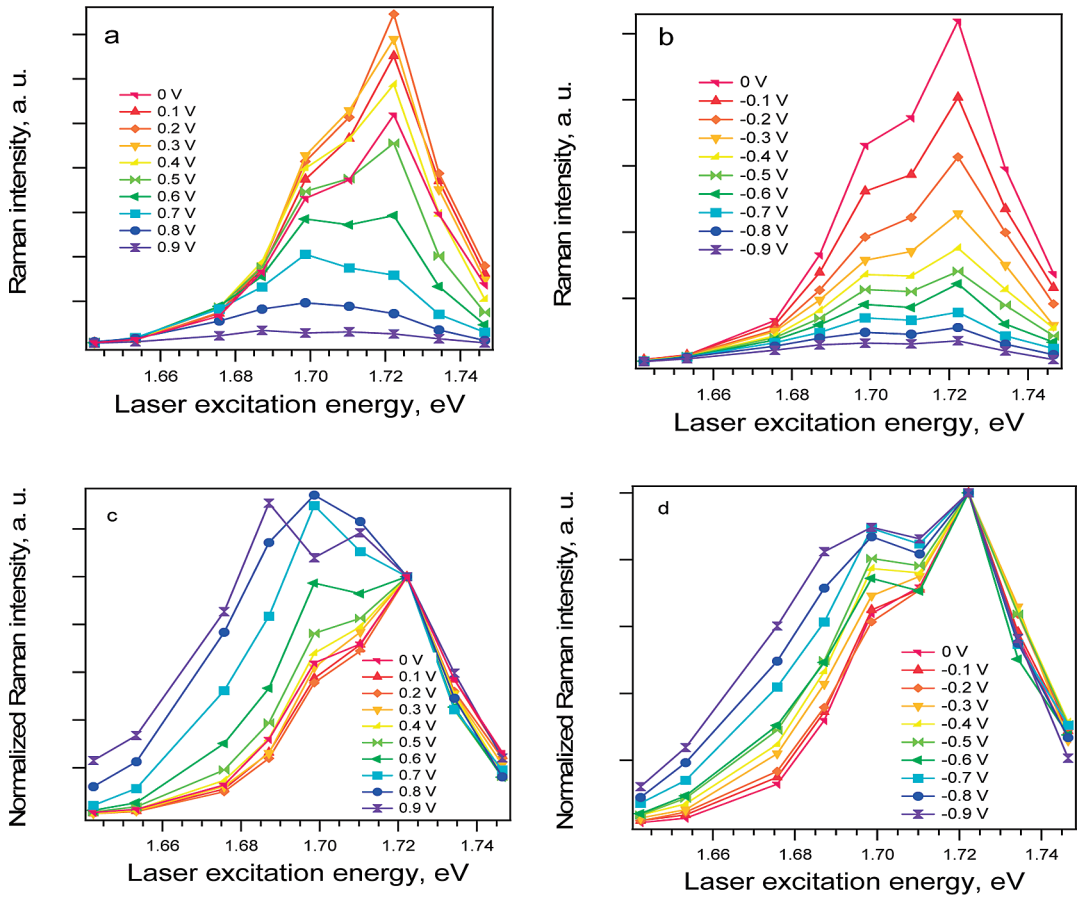

Figure 6. Raman intensity I_{RBM} *vs* laser excitation energy profiles for the metallic (M) tube for positive potentials (a) and for negative potentials (b). The normalized Raman intensity I_{RBM} *vs* laser excitation energy profiles for the metallic (M) tube for positive potentials (c) and for negative potentials (d), in which the Raman intensity for each curve is normalized to I_{RBM} at 1.722 eV.

same time, our present results confirm that the change of E_{ii}^{S} is not a dominant reason for the bleaching of the Raman signal.

As mentioned above, our present results also indicate that the resonance Raman profile is broadened as the magnitude of the electrode potential is increased. This could be a consequence of the broadening of the van Hove singularities/excitonic levels during electrochemical charging. If the van Hove singularity, which corresponds to the E_{ii}^{S} that is in resonance with the laser excitation energy, is broadened, the signal should be decreased since the density of states at this particular singularity would be reduced. Our explanation is also consistent with observations on nanotube bundles with a broad diameter distribution since the van Hove singularities would then be broadened for all tubes, and bleaching of the Raman signal would only be expected as the magnitude of electrode potential is increased.

Figure 6 shows the Raman resonance profiles (panels a and b) and normalized Raman resonance profiles (panels c and d) as a function of E_{laser} for the metallic tube (M). The metallic tube exhibits significant broadening of the resonance profile as the magnitude of the electrode potential is increased. There is also a shift of the resonance maxima to lower energies, which is even larger than in case of semiconducting SWCNTs. We suggest that for semiconducting tubes the change of E_{ii} may be partly compensated by a simultaneous change of the exciton binding energy. For metallic tubes, the effect of the exciton is not present or is much weaker and therefore a stronger shift of the resonant maxima can be rationalized.

The broadening of resonance profile is a major finding of the present work. Therefore, we analyzed the broadening in more detail. The full width at half-maximum (fwhm) line width was evaluated for each curve in Figure 6c,d. A plot of the dependence of the fwhm on the electrode potential is then shown on Figure 7. Note that the fwhm was evaluated neglecting possible two peak structures contained within the curves in Figures 5c,d and 6c,d. An obvious trend seen in Figure 7 is an increase in the fwhm line width with increasing magnitude of the electrode potential. The increase of the fwhm with V_e is gradual, which is consistent with a broadening that depends on the amount of doping-induced charge carriers. For the semiconduct-

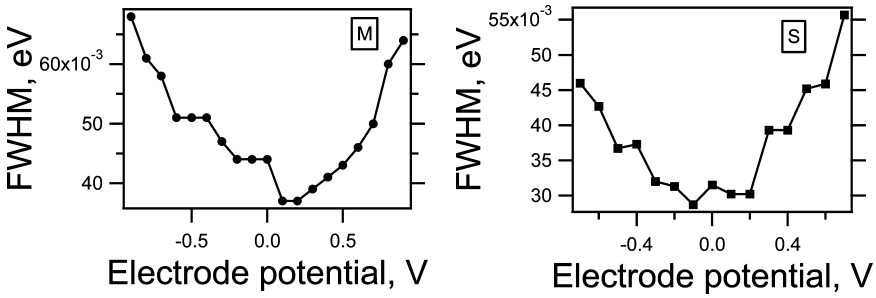

Figure 7. Plot of the dependence of the fwhm of the normalized Raman intensity I_{RBM}/laser excitation energy profiles on electrode potential (left) for the metallic tube (M) and (right) for the semiconducting tube (S) studied in the present work.

ing tube, there is an offset in electrode potential in Figure 7 before the broadening begins to be significant, which is consistent with the results of Figure 3.

For both the semiconducting and metallic tube, the broadening is steeper for positive charging. This is consistent with the bleaching behavior of the I_{RBM} which is also more pronounced for positive doping. Both profiles also exhibit asymmetry with respect to the maximum intensity, which is consistent with our general expectation that the energy bandwidth for the π^* band is larger than that for the π band. The value of the fwhm at $V_e = \pm 0.9$ V is nearly twice as large as the minimum value of the fwhm which occurs at about $V_e = 0.2$ V.

The shift of the maxima of the resonance profile in Figures 5 and 6 to lower E_{laser} energies at high anodic potentials (0.7−0.9 V) is also clearly seen. Furthermore, for the metallic tube, the shift of the resonance maximum is continuous and presumably results in developing a new peak at about 1.70 eV (Figure 6). On the other hand, for the case of the semiconducting tube, the resonance profiles in Figure 5 hardly change until V_e reaches 0.4 or −0.3 V for positive and negative V_e, respectively, and we observed an abrupt shift of the resonance maximum at positive potentials from 0.7 to 0.8 V. For negative potentials, there is a shift of the maximum in I_{RBM} for the M tube (Figure 6b,d), but in contrast, no significant shift is seen for the S tube (Figure 5b,d).

The two peak structure of the resonance profile in Figures 5 and 6 might result simply from the conditions of the resonance with the incident or scattered photon since the peak separation, 0.02 eV, is close to the energy of the RBM phonon. In Figure 8, we show the resonance profile as a function of V_e for the metallic nanotube for 1.70 and 1.72 eV laser energy values. Although the I_{RBM} Raman intensity values scatter as a function of V_e, we can say that the peak I_{RBM} position for $E_{laser} = 1.70$ and 1.72 eV is the same within the experimental error bar, which confirms that E_{ii} does not change much as a function of V_e. It is significant that both peaks in I_{RBM} are bleached with a similar profile as a function of electrode potential, though the I_{RBM} intensity maxima for the two curves are quite different.

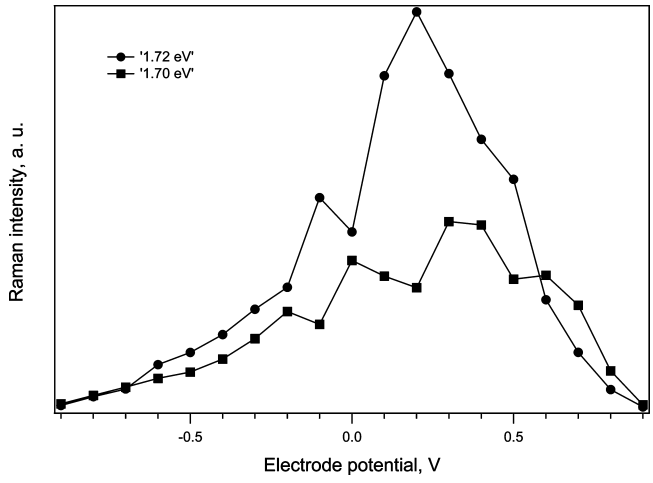

Figure 8. Plot of the dependence of the I_{RBM} intensity of the peaks at 1.70 and 1.72 eV on electrode potential. These peaks were obtained by fitting the curves in Figures 6a,b with two Lorentzian line shape components.

The broadening of the van Hove singularities or of the excitonic states with an increase in the magnitude of V_e may be understood by two possible explanations. One possible reason is a special effect of the RBM mode. The excitation of the RBM phonons induces a radial atomic motion which modifies the E_{ii} values because the E_{ii} values are inversely proportional to the diameter. Thus, the RBM vibration itself broadens the E_{ii} values. The change of E_{ii} by the RBM vibration is generally independent of the RBM phonon energy. However, when the change of E_{ii} matches the RBM phonon energy, we expect a resonance effect which enhances the Raman intensity. This resonance effect is different from the concept of incident and scattered resonance conditions. In fact, this special resonance occurs only for the RBM in a nanotube since the atomic displacements associated with other phonon modes, such as the G band, vibration does not change E_{ii}. This special resonance effect on the RBM may depend on doping, which is relevant to an E_F dependence of the broadening. The other possibility for the broadening is due to the screening or the additional Coulomb interaction between the e−h pair and doped carriers. The real part of this interaction is generally understood by an energy shift of the exciton energy E_{ii} which is commonly observed in the different case of an environmental effect in which the dielectric response from a surfactant changes E_{ii} by up to 50 meV.[27] However, in electrochemical doping, we expect that the real part of the Coulomb interaction should be much smaller than that for the environmental effect. On the other hand, the imaginary part of the Coulomb interaction, which is generally known as the Coulomb interaction energy, makes the lifetime of the exciton states shorter, and this shortened lifetime corresponds to the broadening of the excitonic levels. From a previous calculation of the

exciton, we know that the self-energy of the exciton is proportional to $|E_F|$,[28] which is consistent with the present experimental results that the broadening occurs for both positive and negative values of V_e. On the other hand, a broadening will decrease the band gap. A further investigation of these effects will be reported elsewhere.

CONCLUSION

In conclusion, we used I_{RBM} as a probe to examine the effects of filling and emptying of the electronic states of S and M tubes. An electrode potential applied to the tubes was used to fill/deplete electronic states. We show that the bleaching of the I_{RBM} during application of an electrode potential V_e is indeed related to the depleting/filling of valence and conduction electronic states. This bleaching results from a change in the carrier density of the SWCNT. However, these particular states may lie below the energy of the van Hove singularity, which is employed in the resonance enhancement of the Raman spectra. There is a striking difference between the Raman intensity *versus* potential profiles between metallic and semiconducting tubes. For a metallic tube, the intensity of the Raman signal is already attenuated at potentials that deviate only slightly from $V_e = 0$ V since state filling/depleting can already start at $E_F = 0$ in this case. In contrast, for a semiconducting tube, the Raman intensity is significantly attenuated only after the electrode potential reaches the first van Hove singularity. This is a fundamental difference between semiconducting and metallic tubes, and thus the I_{RBM} *versus* potential profiles might be used to distinguish between metallic and semiconducting tubes.

We also show that the effect of charging on I_{RBM} and on the resonance enhancement of the spectra is significantly dependent on the laser excitation energy. The effect of nanotube charging on I_{RBM} is the strongest for a laser excitation energy which matches the maximum intensity within the resonance window of a given tube. If the laser energy deviates slightly from the maximum of the resonance window, the bleaching of I_{RBM} changes more slowly with V_e. In other words, the resonance window is broadened by the charging of a SWCNT. In particular, this effect is very strong for the metallic tube. This broadening of the resonance window is very important since there is always some natural doping in SWCNT samples. Since the resonance profile of the SWCNT is dependent on doping, different resonance Raman enhancement may be obtained for the same SWCNT in different nanotube samples due to different levels of doping of the probed tube.

The broadening of the resonance profile is suggested to be a consequence of the broadening of van Hove singularities/excitonic levels due to electrochemical charging. The broadening of van Hove singularities/excitonic levels is consistent with bleaching of the RBM Raman intensity signal, and it is believed to be the most important reason for the change of the resonance enhancement during electrochemical charging. Some change in E_{ii} is also observed, but its effect on the bleaching behavior of the Raman signal is minor.

The change of the resonance profile also has important practical consequences as, for example, on the quantitative determination of the amount of a given (n,m) tube that is contained within a given nanotube sample. This is because the presence of carriers will have a different effect on the I_{RBM} at different laser excitation energies. For example, the I_{RBM} of a metallic tube for which the laser is close to its maximum in the resonance profile will be strongly bleached by natural doping, and thus the amount of this particular nanotube present in a given sample when evaluated on the basis of a measurement of the I_{RBM} might be strongly underestimated if, for example, the SWCNTs are doped by oxygen in the air.

EXPERIMENTAL SECTION

SWCNTs were synthesized directly on a SiO_2/Si substrate using Fe as a catalyst. For the electrochemical charging experiments, SWCNTs were directly grown on the substrate, which was subsequently contacted using Au evaporated on a part of the substrate, and served as a working electrode. The cell was completed with a Pt counter electrode and a Ag wire pseudoreference electrode. The electrolyte gel was 0.1 M $LiClO_4$ dissolved in dry propylenecarbonate/PMMA (PMMA = polymethylmethacrylate, Aldrich). Electrochemical charging of the working electrode on which SWCNTs were placed was carried out by varying the applied potential V_e between −1.5 and 1.5 V *versus* a Ag pseudoreference electrode (PAR potentiostat). Note that we used a three-electrode system and measure in the potentiostatic regime, hence no current is flowing during the measurement through the reference electrode. Consequently, the environment of the pseudoreference electrode is not changed during the measurement, and a stable potential of our pseudoreference electrode is ensured.

The Raman spectra were excited by a dye laser (R6G dye, Coherent), a Ti:sapphire laser (Coherent), or a Nd:YAG laser (Coherent). The spectrometer resolution was about 5 cm^{-1}. The spectrometer was interfaced with a microscope (Carl-Zeiss, objective 100×). The diameter of the laser spot was about 0.5 μm.

Acknowledgment. This work was supported by the Academy of Sciences of the Czech Republic (Contracts Nos. 203/07/J067, IAA400400804, IAA400400911, and KAN200100801), MSMT (ME09060). M.S.D. acknowledges support from NSF/DMR-07-04197; H.F. and J.K. acknowledge support from the Materials, Structure and Devices Center, one of the five programs in the focus center research program (FCRP). K.S. acknowledges a Grant-in-Aid for Specially Promoted Research (No. 20001006) from MEXT. R.S. acknowledges MEXT Grant No. 20241023. Work was carried out using the Raman facility in the MIT Spectroscopy Laboratory supported by Grant Nos. NSF-CHE 0111370 and NIH-RR02594.

REFERENCES AND NOTES

1. Rao, A. M.; Eklund, P. C.; Bandow, S.; Thess, A.; Smalley, R. E. Evidence for Charge Transfer in Doped Carbon Nanotube Bundles From Raman Scattering. *Nature* **1997**, *388*, 257–259.
2. Tsang, J. C.; Freitag, M.; Perebeinos, V.; Liu, J.; Avouris, P. Doping and Phonon Renormalization in Carbon Nanotubes. *Nat. Nanotechnol.* **2007**, *2*, 725–730.
3. Das, A.; Sood, A. K.; Govindaraj, A.; Saitta, A. M.; Lazzeri, M.; Mauri, F.; Rao, C. N. R. Probing the Doping in Metallic and Semiconducting Carbon Nanotubes by Raman and Transport Measurements. *Phys. Rev. Lett.* **2007**, *99*, 136803.
4. Farhat, H.; Son, H.; Samsonidze, G. G.; Reich, S.; Dresselhaus, M. S.; Kong, J. Phonon Softening in Individual Metallic Carbon Nanotubes Due to the Kohn Anomaly. *Phys. Rev. Lett.* **2007**, *99*, 145506.
5. Kalbac, M.; Farhat, H.; Kavan, L.; Kong, J.; Dresselhaus, M. S. Competition between the Spring Force Constant and the Phonon Energy Renormalization in Electrochemically Doped Semiconducting Single Walled Carbon Nanotubes. *Nano Lett.* **2008**, *8*, 3532–3537.
6. Heller, I.; Kong, J.; Williams, K. A.; Dekker, C.; Lemay, S. G. Electrochemistry at Single-Walled Carbon Nanotubes: The Role of Band Structure and Quantum Capacitance. *J. Am. Chem. Soc.* **2006**, *128*, 7353–7359.
7. Rafailov, P. M.; Thomsen, C.; Dettlaff-Weglikowska, U.; Roth, S. High Levels of Electrochemical Doping of Carbon Nanotubes: Evidence for a Transition From Double-Layer Charging to Intercalation and Functionalization. *J. Phys. Chem. B* **2008**, *112*, 5368–5373.
8. Okazaki, K.; Nakato, Y.; Murakoshi, K. Characteristics of Raman Features of Isolated Single-Walled Carbon Nanotubes under Electrochemical Potential Control. *Surf. Sci.* **2004**, *566*, 436–442.
9. Kavan, L.; Dunsch, L. Spectroelectrochemistry of Carbon Nanostructures. *ChemPhysChem* **2007**, *8*, 975–998.
10. Kalbac, M.; Kavan, L.; Zukalova, M.; Dunsch, L. Two Positions of Potassium in Chemically Doped C-60 Peapods: An *In Situ* Spectroelectrochemical Study. *J. Phys. Chem. B* **2004**, *108*, 6275–6280.
11. Maultzsch, J.; Reich, S.; Thomsen, C. Double-Resonant Raman Scattering in Graphite: Interference Effects, Selection Rules, and Phonon Dispersion. *Phys. Rev. B* **2004**, *70*, 155403.
12. Thomsen, C.; Reich, S. Double Resonant Raman Scattering in Graphite. *Phys. Rev. Lett.* **2000**, *85*, 5214–5217.
13. Araujo, P. T.; Doorn, S. K.; Kilina, S.; Tretiak, S.; Einarsson, E.; Maruyama, S.; Chacham, H.; Pimenta, M. A.; Jorio, A. Third and Fourth Optical Transitions in Semiconducting Carbon Nanotubes. *Phys. Rev. Lett.* **2007**, *98*, 067401.
14. Araujo, P. T.; Maciel, I. O.; Pesce, P. B. C.; Pimenta, M. A.; Doorn, S. K.; Qian, H.; Hartschuh, A.; Steiner, M.; Grigorian, L.; Hata, K.; Jorio, A. Nature of the Constant Factor in the Relation between Radial Breathing Mode Frequency and Tube Diameter for Single-Wall Carbon Nanotubes. *Phys. Rev. B* **2008**, *77*, 241403.
15. Rafailov, P. M.; Maultzsch, J.; Thomsen, C.; Kataura, H. Electrochemical Switching of the Peierls-like Transition in Metallic Single-Walled Carbon Nanotubes. *Phys. Rev. B* **2005**, *72*, 045411.
16. Corio, P.; Jorio, A.; Demir, N.; Dresselhaus, M. S. Spectro-Electrochemical Studies of Single Wall Carbon Nanotubes Films. *Chem. Phys. Lett.* **2004**, *392*, 396–402.
17. Kalbac, M.; Kavan, L.; Dunsch, L.; Dresselhaus, M. S. Development of the Tangential Mode in the Raman Spectra of SWCNT Bundles During Electrochemical Charging. *Nano Lett.* **2008**, *8*, 1257–1264.
18. Paolucci, D.; Franco, M. M.; Iurlo, M.; Marcaccio, M.; Prato, M.; Zerbetto, F.; Penicaud, A.; Paolucci, F. Singling out the Electrochemistry of Individual Single-Walled Carbon Nanotubes in Solution. *J. Am. Chem. Soc.* **2008**, *130*, 7393–7399.
19. Cronin, S. B.; Barnett, R.; Tinkham, M.; Chou, S. G.; Rabin, O.; Dresselhaus, M. S.; Swan, A. K.; Unlu, M. S.; Goldberg, B. B. Electrochemical Gating of Individual Single-Wall Carbon Nanotubes Observed by Electron Transport Measurements and Resonant Raman Spectroscopy. *Appl. Phys. Lett.* **2004**, *84*, 2052–2054.
20. Rafailov, P. M.; Jantoljak, H.; Thomsen, C. Electronic Transitions in Single-Walled Carbon Nanotubes: A Resonance Raman Study. *Phys. Rev. B* **2000**, *61*, 16179–16182.
21. O'Connell, M. J.; Sivaram, S.; Doorn, S. K. Near-Infrared Resonance Raman Excitation Profile Studies of Single-Walled Carbon Nanotube Intertube Interactions: A Direct Comparison of Bundled and Individually Dispersed HiPco Nanotubes. *Phys. Rev. B* **2004**, *69*, 235415.
22. Sasaki, K. I.; Saito, R.; Dresselhaus, G.; Dresselhaus, M. S.; Farhat, H.; Kong, J. Chirality-Dependent Frequency Shift of Radial Breathing Mode in Metallic Carbon Nanotubes. *Phys. Rev. B* **2008**, *78*, 235405.
23. Weisman, R. B.; Bachilo, S. M. Dependence of Optical Transition Energies on Structure for Single-Walled Carbon Nanotubes in Aqueous Suspension: An Empirical Kataura Plot. *Nano Lett.* **2003**, *3*, 1235–1238.
24. Kataura, H.; Kumazawa, Y.; Maniwa, Y.; Umezu, I.; Suzuki, S.; Ohtsuka, Y.; Achiba, Y. Optical Properties of Single-Wall Carbon Nanotubes. *Synth. Met.* **1999**, *103*, 2555–2558.
25. Tarabek, J.; Kavan, L.; Dunsch, L.; Kalbac, M. Chemical States of Electrochemically Doped Single Wall Carbon Nanotubes as Probed by *In Situ* Raman Spectroelectrochemistry and *Ex Situ* X-ray Photoelectron Spectroscopy. *J. Phys. Chem. C* **2008**, *112*, 13856–13861.
26. Saito, R.; Dresselhaus, G.; Dresselhaus, M. S. *Physical Properties of Carbon Nanotubes*; Imperial College Press: London, 1998.
27. Miyauchi, Y.; Saito, R.; Sato, K.; Ohno, Y.; Iwasaki, S.; Mizutani, T.; Jiang, J.; Maruyama, S. Dependence of Exciton Transition Energy of Single-Walled Carbon Nanotubes on Surrounding Dielectric Materials. *Chem. Phys. Lett.* **2007**, *442*, 394–399.
28. Sato, K.; Saito, R.; Jiang, J.; Dresselhaus, G.; Dresselhaus, M. S. Discontinuity in the Family Pattern of Single-Wall Carbon Nanotubes. *Phys. Rev. B* **2007**, *76*, 195446.